Thrombospondin-1 Is a Major Activator of TGF-β Signaling in Recessive Dystrophic Epidermolysis Bullosa Fibroblasts

Velina S. Atanasova[1], Rebecca J. Russell[1], Timothy G. Webster[1], Qingqing Cao[1], Pooja Agarwal[2], Yok Zuan Lim[1], Suma Krishnan[2], Ignacia Fuentes[1,3], Christina Guttmann-Gruber[4], John A. McGrath[5], Julio C. Salas-Alanis[6], Andrzej Fertala[7] and Andrew P. South[1]

Mutations in the gene encoding collagen VII cause the devastating blistering disease recessive dystrophic epidermolysis bullosa (RDEB). RDEB is characterized by severe skin fragility and nonhealing wounds aggravated by scarring and fibrosis. We previously showed that TSP1 is increased in RDEB fibroblasts. Because transforming growth factor-β (TGF-β) signaling is also increased in RDEB, and TSP1 is known to activate TGF-β, we investigated the role of TSP1 in TGF-β signaling in RDEB patient cells. Knockdown of TSP1 reduced phosphorylation of smad3 (a downstream target of TGF-β signaling) in RDEB primary fibroblasts, whereas overexpression of collagen VII reduced phosphorylation of smad3. Furthermore, inhibition of TSP1 binding to the LAP/TGF-β complex decreased fibrosis in engineered extracellular matrix formed by RDEB fibroblasts, as evaluated by picrosirius red staining and analyses of birefringent collagen fibrillar deposits. We show that collagen VII binds TSP1, which could potentially limit TSP1-LAP association and subsequent TGF-β activation. Our study suggests a previously unreported mechanism for increased TGF-β signaling in the absence of collagen VII in RDEB patient skin. Moreover, these data identify TSP1 as a possible target for reducing fibrosis in the tumor-promoting dermal microenvironment of RDEB patients.

INTRODUCTION

Tissue repair after injury is a complex and highly regulated process that juxtaposes extracellular matrix (ECM) deposition and remodeling with inflammatory cascades (Diegelmann and Evans, 2004). Perturbation of these processes results in pathological outcomes, such as chronic nonhealing wounds or excessive fibrosis, leading to scarring and tissue contracture. In the skin, the fibrillar collagen, collagen VII (C7), is important for wound healing (Nyström et al., 2013). We and others have shown that loss of C7, either in primary cells with germline loss-of-function mutations in the gene encoding C7 (from patients with recessive dystrophic epidermolysis bullosa [RDEB]) or after small interfering RNA knockdown of COL7A1 in normal cells, results in global changes to composition of the ECM secreted by dermal fibroblasts (Kuttner et al., 2013; Ng et al., 2012). Indeed, RDEB, which is caused by loss-of-function mutations in C7, is a paradigm of injury and inflammation-driven soft tissue fibrosis (Nyström and Bruckner-Tuderman, 2018).

RDEB is characterized by trauma-induced blistering and chronic wounds leading to progressive scarring, joint contractures, esophageal strictures, and mutilating fusion of the digits in both the hands and feet. The fibrotic microenvironment predisposes RDEB patients to develop aggressive and frequently fatal squamous cell carcinomas (SCCs) (Fine et al., 2009; Mittapalli et al., 2016; Ng et al., 2012). Although it has been shown that increased transforming growth factor (TGF)-β signaling is downstream of C7 loss (Fritsch et al., 2008; Kuttner et al., 2014; Ng et al., 2012; Odorisio et al., 2014) and that indirect inhibition of this pathway has remarkable preclinical efficacy in animal models (Nyström et al., 2015), little work has characterized the mechanisms by which TGF-β is activated in RDEB, a process that typically requires enzymatic or mechanical liberation of this growth factor from ECM-bound complexes. One prominent activator of TGF-β is the matricellular protein TSP1 (Ribeiro et al., 1999), which binds to LAP and induces conformational change to release the TGF-β ligand (Schultz-Cherry et al., 1994a, 1994b; Schultz-Cherry et al., 1995). TSP1-knockout animals phenocopy TGF-β1−knockout animals, suggesting that absence of TSP1 has similar effect to absence of TGF-β1 in vivo (Crawford et al., 1998; Daniel et al., 2007).

TSP1 is a homotrimeric glycoprotein that is secreted from platelet α-granules and incorporated into fibrin clots in

[1]Department of Dermatology and Cutaneous Biology, Thomas Jefferson University, Philadelphia, Pennsylvania, USA; [2]Krystal Biotech Inc., Pittsburgh, Pennsylvania, USA; [3]Fundación DEBRA Chile, Santiago, Chile; [4]EB House Austria, Research Program for the Molecular Therapy of Genodermatoses, Department of Dermatology, University Hospital of the Paracelsus Medical University Salzburg, Salzburg, Austria; [5]St. John's Institute of Dermatology, King's College London (Guy's Campus), London, UK; [6]Instituto Dearmatologico de Jalisco, Guadalajara, Mexico; and [7]Department of Orthopedics, Thomas Jefferson University, Philadelphia, Pennsylvania, USA

Correspondence: Department of Dermatology and Cutaneous Biology, Thomas Jefferson University, 406 Bluemle Life Sciences Building, Philadelphia, Pennsylvania 19107, USA. E-mail: Andrew.South@Jefferson.edu

ARTICLE IN PRESS

VS Atanasova et al.
C7, TSP1, and TGF-β Activation in RDEB

response to injury (Agah et al., 2002; DiPietro et al., 1996; Murphy-Ullrich and Mosher, 1985; Raugi et al., 1987). Apart from this normal physiological function, TSP1 is often overexpressed in fibrotic and tumor-promoting tissue environments (Castle et al., 1991; Hugo, 2003; Wang et al., 1995), and TSP1 plays an important role in wound repair and healing, as shown by studies in mice overexpressing TSP1 that have delayed wound healing (DiPietro et al., 1996; Streit et al., 2000). Furthermore, yeast two-hybrid analysis previously identified that the FN6-FN7 repeats in the C7 NC1 domain potentially interact with the TSP1 type I repeat region, the site identified for binding LAP (Aho and Uitto, 1998; Schultz-Cherry et al., 1994a). Because we and others have reported increased TSP1 in RDEB fibroblasts and skin, and increased TSP1 after knockdown of C7 in normal fibroblasts (Kuttner et al., 2014; Martins et al., 2016; Ng et al., 2012; Nyström et al., 2013), we investigated the role of TSP1 in TGF-β activation in RDEB.

RESULTS

TGF-β and TSP1 are increased in RDEB
In agreement with existing data (Fritsch et al., 2008; Kuttner et al., 2013, 2014; Martins et al., 2016; Ng et al., 2012; Nyström et al., 2013, 2015), increased TGF-β signaling (as determined by increased phosphorylation of smad3, a downstream target of TGF-β) and increased expression of TSP1 were evident in the primary RDEB fibroblasts used in this study (Figure 1a and b). The level of phosphorylated smad3 showed a positive correlation with the level of TSP1 in primary RDEB fibroblasts (Figure 1c). Re-expression of C7 in RDEB fibroblasts resulted in a significant decrease in intracellular TSP1 protein and a corresponding increase in secreted TSP1 (Figure 1d, left panels) in the absence of immediate change to overall TSP1 transcript levels (Figure 1d, right panels).

Small interfering RNA depletion of TSP1 down-regulates TGF-β signaling in RDEB fibroblasts but not in normal fibroblast controls
To investigate the role of TSP1 in TGF-β activation in dermal RDEB fibroblasts, we first used small interfering RNA to transiently knock down TSP1. After 48 hours of TSP1 knockdown, there was significant down-regulation of phosphorylated smad3 levels in the RDEB cells but not in the normal controls (Figure 2a). In some RDEB primary cell populations, down-regulation of the TGF-β pathway after TSP1 decrease was comparable to that found in cells treated with the TGF-β receptor I inhibitor SB431542 (Halder et al., 2005) (Figure 2a).

Next, we overexpressed C7 in normal and RDEB fibroblasts and showed that recombinant C7 reduced both intracellular TSP1 levels and TGF-β signaling in RDEB fibroblasts, and not in controls (Figure 2b). Collectively, these data show that changes to TSP1 protein specifically dictate TGF-β signaling in RDEB fibroblasts, whereas this pathway in normal dermal fibroblasts remains unaffected after manipulation of either C7 or TSP1.

C7 binds TSP1
In vitro studies using two-hybrid methodology have suggested that C7 can bind TSP1 in the same domain of TSP1 that has been shown to bind LAP (Aho and Uitto, 1998; Schultz-Cherry

et al., 1994a). To confirm and extend these data to primary human cells, we used three separate approaches to investigate the binding interactions between C7 and TSP1. First, we performed the proximity ligation assay using antibodies against C7 and TSP1 and showed a strong positive intracellular signal in normal dermal fibroblasts that was absent in RDEB fibroblasts and single antibody controls (Figure 3a), indicating that in the normal fibroblasts these two proteins are in close proximity (<30 nm). Next, we confirmed binding of C7 and TSP1 in human fibroblasts using co-immunoprecipitation after delivery of recombinant, tagged C7 to RDEB primary fibroblasts via viral transfer (Figure 3b). To analyze the kinetics of C7-TSP1 binding in real time, we used a label-free approach to analyze binding interactions of recombinant TSP1 and untagged C7. Using immobilized C7 or TSP1, we showed that the affinity of C7 for TSP1 (calculated from the equilibrium association constant values, see Materials and Methods) is $7.3 \times 10^6 \, M^{-1}$, a value that is substantially greater than the affinity of another basement membrane-associated collagen shown to bind TSP1 (Galvin et al., 1987), collagen IV ($2.2 \times 10^3 \, M^{-1}$), (Figure 3c and Table 1). TSP1 affinity for MMP9, shown to also bind TSP1 type I repeats, was greater than C7 (Bein and Simons, 2000; Rodriguez-Manzaneque et al., 2001), recording an equilibrium constant value of $3.5 \times 10^7 \, M^{-1}$ (Figure 3c and Table 1). Using this approach, we were unable to show binding between TSP1 and commercially available LAP (data not shown).

Fibrosis in RDEB can be modeled by tissue engineered from fibroblasts in suspension culture
To model pathological ECM derived from RDEB fibroblasts, we adapted a previous approach used to identify differences in the tumor-promoting properties of RDEB fibroblasts (Ng et al., 2012; Ng and South, 2014). This assay uses ECM secreted by primary fibroblasts over a number of weeks and was used previously to identify the tumor-inhibitory effects of C7 in three-dimensional invasion assays (Ng et al., 2012). Here, we adapted this assay to measure collagen density and fibril thickness as parameters describing fibrosis (see Supplementary Figure S1a online). Initial quantification of collagen birefringence at the point of ECM release from rigid tissue culture substrate (day 0) did not show any quantifiable differences between RDEB and normal dermal fibroblasts, whereas ECM engineered from RDEB fibroblasts after 7 days in suspension culture exhibited increased collagen density compared with normal dermal fibroblasts, as determined by quantitation of collagen birefringence after picrosirius red staining and image acquisition using a polarizing microscope (Figure 4a). This difference was consistent across all five RDEB patient-derived fibroblasts tested (Figure 4b). We further investigated the role of TFG-β in the difference between RDEB and normal fibroblast engineered ECM and showed that RDEB matrices were, for the most part, insensitive to TGF-β1 ligand stimulation (see Supplementary Figure 1b), whereas normal dermal fibroblasts exhibited increased collagen density similar to those observed in RDEB across all normal fibroblast populations tested (Figure 4c). Collectively, these data suggest that TGF-β signaling promotes collagen changes in this assay and that, in the majority of RDEB fibroblast populations, TGF-β signaling is saturated.
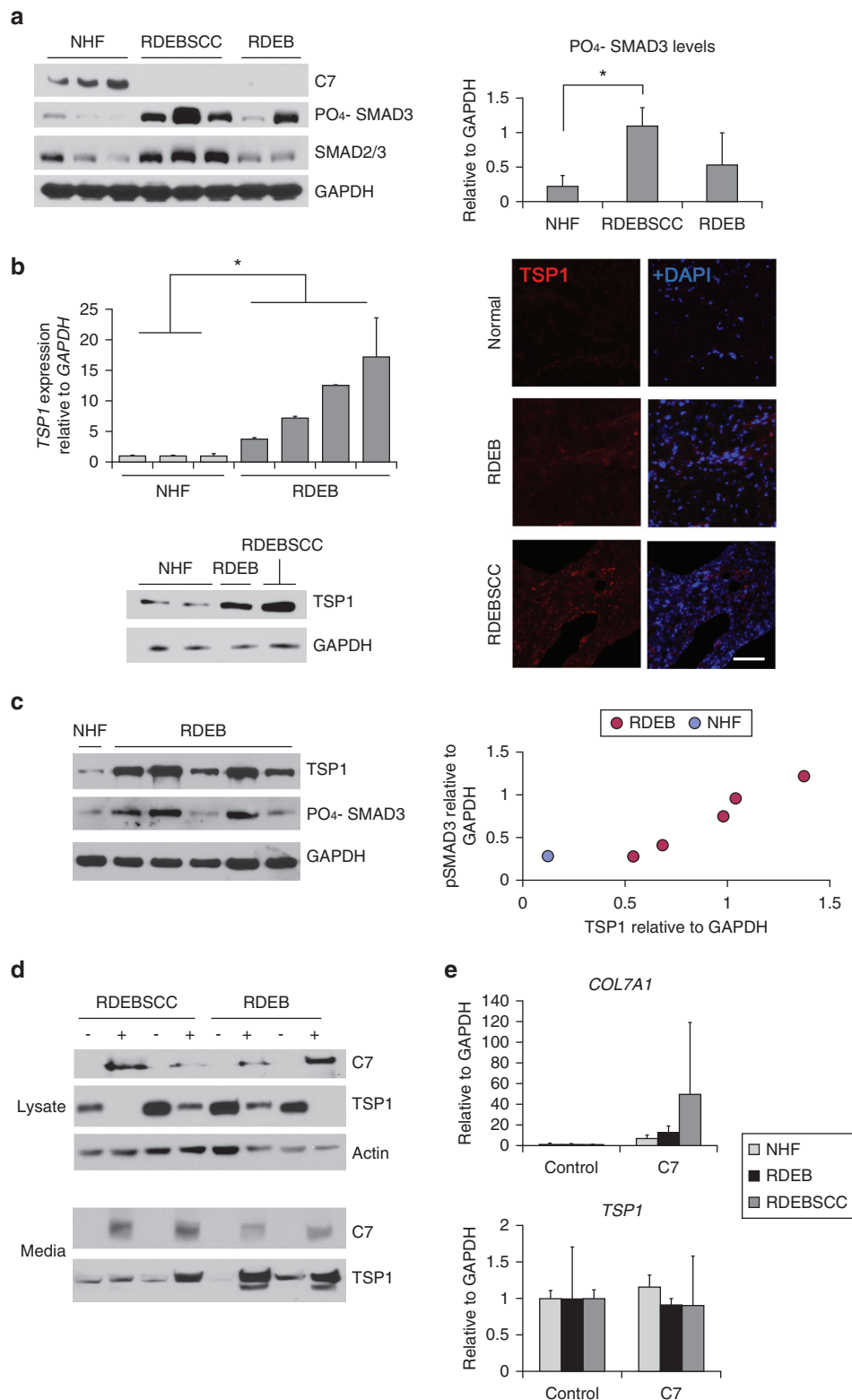
ARTICLE IN PRESS

VS Atanasova et al.
C7, TSP1, and TGF-β Activation in RDEB

Figure 1. TGF-β signaling and TSP1 are up-regulated in RDEB. (**a**) Phosphorylated smad3 (PO$_4$-SMAD3) immunoblotting total lysate from RDEB, RDEB SCC, and normal human fibroblasts. Graph shows densitometry quantification (± standard deviation). (**b**) Graph shows quantitative PCR comparing NHF with RDEB (± standard deviation). Immunoblot compares NHF with RDEB and RDEB SCC. Immunohistochemistry shows a 400-μm region of normal breast dermis, RDEB SCC stroma, and corresponding perilesional dermis (RDEB). Full images and regions are presented in Supplementary Figure S2 online. Scale bar = 100 μm. (**c**) Immunoblot comparing NHF with RDEB. Graph plots the corresponding TSP1 (*x*-axis) quantitation against PO$_4$-SMAD3 (*y*-axis). (**d**) Re-expression of C7 in RDEB decreases intracellular and increases extracellular TSP1 compared with control. (**e**) Graphs show quantitative PCR 48 hours after transduction of NHF (n = 2), RDEB SCC (n = 2), and RDEB (n = 2) (± standard deviation). *$P < 0.05$. For full details of the samples, see the extended legend in the Supplementary Materials online. NHF, normal human fibroblast; RDEB, recessive dystrophic epidermolysis bullosa; SCC, squamous cell carcinoma; TGF, transforming growth factor.

Inhibition of TSP1 binding to LAP−TGF-β reduces collagen fibril deposition in RDEB-derived ECM

To investigate the role of TSP1 in TGF-β activation in RDEB engineered matrices and consequent formation of fibrotic ECM, we inhibited TSP1 using a four-amino acid peptide, LSKL, which prevents binding of TSP1 to the LAP−TGF-β complex and release of the TGF-β ligand (Kuroki et al., 2015; Ribeiro et al., 1999). Previous studies in other disease models have shown that TGF-β activation can be attenuated by inhibition of TSP1 with the LSKL peptide (Kuroki et al., 2015). Treatment with the TSP1 inhibitor peptide LSKL significantly decreased collagen density in RDEB matrices but did not
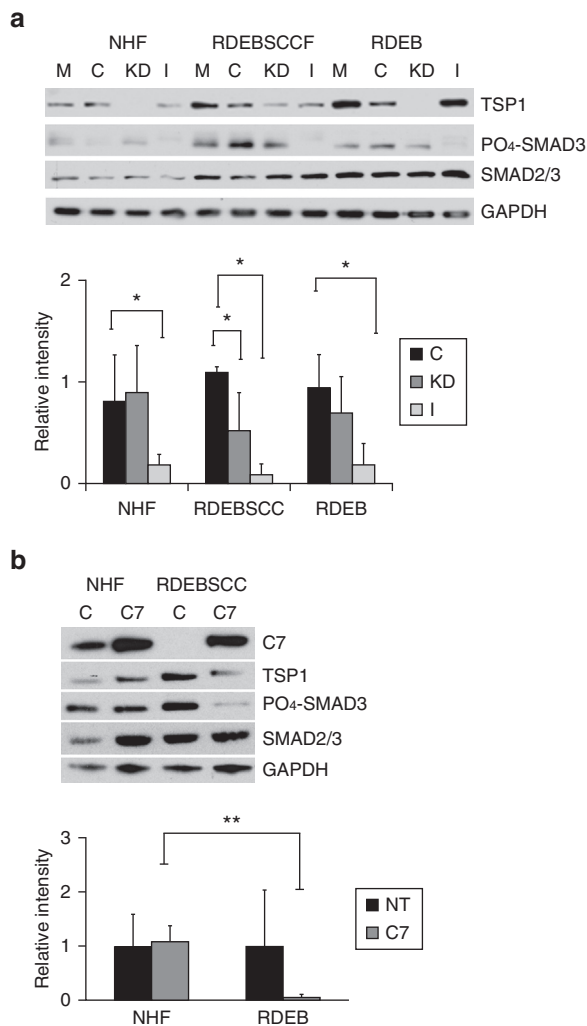
VS Atanasova et al.
C7, TSP1, and TGF-β Activation in RDEB

Figure 2. Phosphorylated smad3 levels are reduced after TSP1 siRNA knockdown or C7 overexpression in RDEB fibroblasts. (**a**) Transient siRNA knockdown of TSP1 (KD) down-regulates TGF-β signaling in RDEB fibroblasts compared with mock transfection (M) or scrambled siRNA control (C). The TGF-βR1 inhibitor SB431542 is used as a positive control (I). Graph shows mean (± standard deviation) quantitation of phosphorylated smad3 (PO₄-SMAD3) levels relative to GAPDH for six independent experiments. Normal human fibroblasts are represented by Br43F, Br46F, and Br48F. RDEBSCC fibroblasts are represented by RDEB70F and RDEB71F, and RDEB fibroblasts are represented by RDEB75F, RDEB81F, and RDEB84F. (**b**) Overexpression of C7 significantly down-regulates TGF-β signaling in RDEB fibroblasts (RDEB70SCCF) but not in normal human fibroblasts Br43F. Graph shows mean (± standard deviation) quantitation of phosphorylated smad3 (PO₄-SMAD3) levels relative to GAPDH for three independent experiments. *$P < 0.05$, **$P < 0.005$. C7, collagen VII; NHF, normal human fibroblast; RDEB, recessive dystrophic epidermolysis bullosa; siRNA, small interfering RNA; TGF, transforming growth factor.

significantly affect collagen deposition in normal cell controls (Figure 4d).

DISCUSSION

Loss of C7 has a significant effect on the expression of matrix proteins and ECM composition. In addition, studies have shown that loss of C7 is associated with increased TGF-β signaling (Kuttner et al., 2013; Ng et al., 2012; Nyström et al., 2013). The profibrotic consequences of the absence of C7 have also been correlated with reduced proteolysis (Kuttner et al., 2013), as well as with altered protein trafficking and autophagy (Kuttner et al., 2014). However, these earlier studies do not offer any mechanistic insight into the consequences of C7 loss. Certainly, a reduction in proteolysis, a mechanism that promotes TGF-β activation through protein cleavage (Sato and Rifkin, 1989; Yu and Stamenkovic, 2000), does not explain increased TGF-β signaling, and although changes to protein trafficking and autophagy will certainly affect the composition of secreted proteins, just how C7 directs these alterations remains unclear. Here, we present data that begin to reveal one mechanism through which C7 loss translates to an increase in TGF-β signaling, by identifying a previously unreported relationship between C7 and TSP1, a known activator of TGF-β. The data presented herein show that C7 binds to TSP1 (Figure 3) at the same site in TSP1 identified to bind to LAP, that reduction of TSP1 in RDEB fibroblasts directly reduces phosphorylation of smad3 (Figure 2a), and that inhibition of TSP1−TGF-β−LAP binding reduces fibrosis in ECM engineered from RDEB fibroblasts (Figure 4). Collectively, these observations lead to a model in normal skin where C7 sequesters TSP1 and prevents it from binding to the LAP−TGF-β complex and activating TGF-β, whereas in RDEB skin, C7 is absent, which leads to both an increase in TSP1 and availability for activating TGF-β (Figure 5). In addition, the data presented here raise a number of important questions, the answers to which will likely increase the complexity of our proposed model. For example, TSP1 levels are increased in RDEB (Ng et al., 2012; Nyström et al., 2013), yet the immediate effects of C7 manipulation do not appear to directly affect TSP1 transcription; rather, the data show changes to TSP1 secretion (Figure 1d). The fact that C7 binds TSP1 intracellularly (Figure 3a) presents the possibility that in dermal fibroblasts, C7 and TSP1 are secreted together. Definitive demonstration of this idea would have an obvious impact on how TSP1 is incorporated into the ECM of normal skin. However, the exact relationship between these two proteins with regard to secretion from the cell is beyond the scope of this study and is an active topic of our investigation. Furthermore, TSP1 expression has been shown to be regulated by numerous signaling pathways and subject to feedback loops at both the transcription and posttranslation levels (reviewed by Zhao et al., 2018). Therefore, just how TSP1 is increased in RDEB remains to be determined.

Whether TSP1-mediated increase in TGF-β signaling occurs in homeostatic RDEB skin or whether it has more relevance after wounding, where the levels of both C7 (Nyström et al., 2013) and TSP1 (Agah et al., 2002) are increased, also remains to be determined, and although the data presented here support the supposition of our model, further work is necessary to validate the exact role of C7-TSP1 binding in activation of TGF-β signaling. One might predict that C7 affinity for TSP1 would be greater than LAP if our model is proven; however, we were unable to determine the affinity of LAP for TSP1 for comparison with the experiments presented here. These data certainly do not rule out direct LAP-TSP1 binding, but they do preclude speculation regarding binding affinities. Our data show that C7 affinity for TSP1 was less
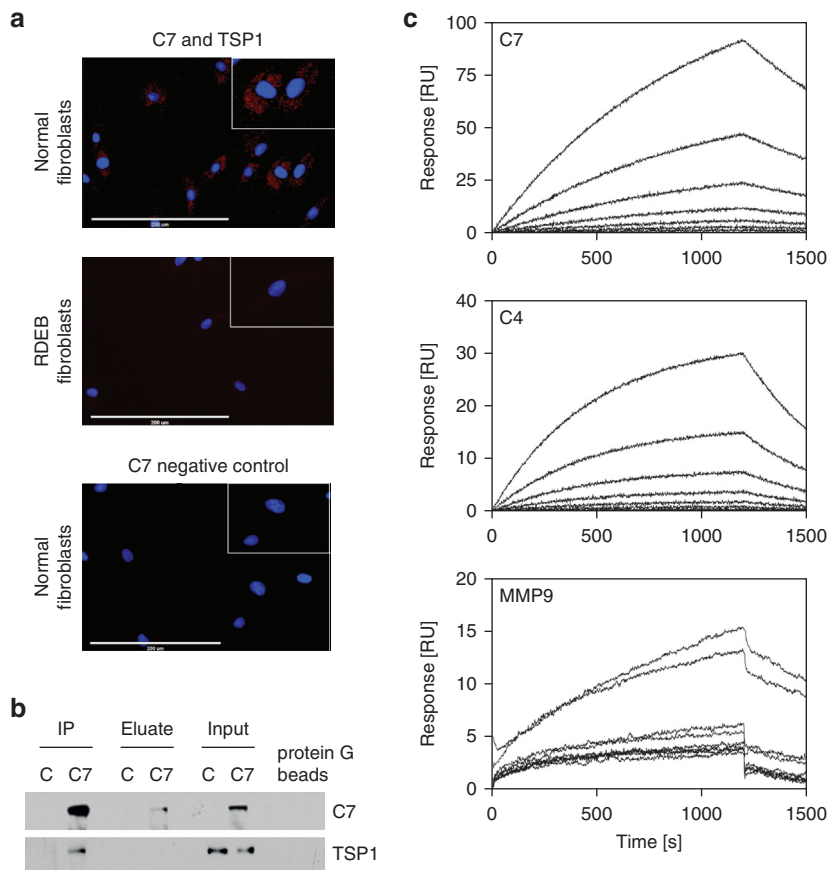
ARTICLE IN PRESS

VS Atanasova et al.
C7, TSP1, and TGF-β Activation in RDEB

a

C7 and TSP1

Normal fibroblasts

RDEB fibroblasts

C7 negative control

Normal fibroblasts

b

	IP		Eluate		Input		
	C	C7	C	C7	C	C7	protein G beads

C7

TSP1

c

Figure 3. **C7 binds TSP1.** (**a**) Proximity ligation assay using normal fibroblasts shows co-localization of C7 and TSP1 intracellularly (left panel), which is absent in RDEB fibroblasts (RDEB75F, lower panel). C7 antibody alone confirms specificity in normal fibroblasts (right panel). Scale bar = 200 μm. (**b**) Co-IP confirms binding between C7 and TSP1. C indicates RDEB75F and C7 indicates RDEB75F expressing C7-DDK. IP (first two lanes) shows the C7 precipitated fraction. Eluate (second two lanes) shows the nonbound fraction. Protein G beads (last lane) show no nonspecific binding to C7 or TSP1. (**c**) Association and dissociation curves illustrating the kinetics of the TSP1/C7, TSP1/collagen IV, and TSP1/MMP9 binding interactions; the curves represent association and dissociation events at various concentrations of free interactants. C7, collagen VII; IP, immunoprecipitation; RDEB, recessive dystrophic epidermolysis bullosa; RU, arbitrary response units.

than the known strong-interacting partners of C7 such as LN332 or collagen IV but was greater than weaker-interacting proteins such as collagen I (Brittingham et al., 2006). Therefore, it is likely that our proposed model is relevant in the absence of close proximity between keratinocytes and fibroblasts, because keratinocytes are the sole source of LN332 and substantially contribute collagen IV. An open, unhealed wound or a fibrotic scar are environments that would have less LN332 and collagen IV available compared with intact, homeostatic skin, and certainly we envisage this mechanism to be of particular importance in a wounded environment and in the context of SCC. Of course, the fact that TSP1 binds a great many other proteins in the ECM (Resovi et al., 2014) will have considerable impact in this context, and it will be important to further study the relationship between TSP1 and C7 in both wounded and SCC environments.

Our experiments have used primary cells isolated from 16 different patients (see Supplementary Table S1), which inevitably leads to some variability in response (Figures 1, 2, and 4). However, this variation lends itself to important observations. The first of these is that the largest delta in our experiments is seen when comparing RDEB fibroblasts isolated from SCC: RDEB SCC fibroblasts have more phosphorylated smad3 (Figure 1a) and show significant reduction in phosphorylated smad3 after TSP1 knockdown (Figure 2a). These data agree with our earlier mRNA studies showing that the greatest delta in gene expression differences between normal, RDEB, and RDEB SCC fibroblasts are seen in RDEB SCC (Ng

et al., 2012). Our second observation is that re-expression of C7 has a greater effect on phosphorylation of smad3 when compared with TSP1 knockdown (Figure 2). We speculate two possible explanations for this. The first is that variation in lipid transfection efficiencies, which can potentially reduce the consistency of TSP1 knockdown and C7 overexpression by means of viral transduction, is more reproducible, resulting in more consistent data. Although this remains a possibility, we observe reproducibility within individual patient populations, and we prefer a second explanation: that disease modifiers exist independent of TSP1 and that the full extent of the role of C7 in maintaining dermal architecture remains to be determined. In this respect, a study of monozygotic twins, in which the more severely affected sibling had increased evidence of TGF-β signaling, identified the TGF-β pathway inhibitor decorin as being increased in the less affected sibling (Odorisio et al., 2014). Decorin has been shown to bind both TSP1 and LAP–TGF-β (Merle et al., 1997; Yamaguchi et al., 1990), and therefore an increase in

Table 1. Summary of the binding kinetics

Binding Interaction	k_{on} ($M^{-1}s^{-1}$)	k_{off} (s^{-1})	K_d (M)	K_a (M^{-1})
TSP1/C7	7.12×10^3	9.76×10^{-4}	1.4×10^{-7}	7.3×10^6
TSP1/collagen IV	4.80	2.15×10^{-3}	4.5×10^{-4}	2.2×10^3
TSP1/MMP9	3.70×10^4	1.07×10^{-3}	2.9×10^{-8}	3.5×10^7

Abbreviation: M, mol/L.

ARTICLE IN PRESS

VS Atanasova et al.
C7, TSP1, and TGF-β Activation in RDEB

Figure 4. RDEB engineered ECM exhibits increased collagen density compared with normal ECM and can be reduced using a peptide inhibitor of TSP1-LAP binding. (**a**) Bar graph shows mean relative green or red pixel intensity (± standard deviation) of images of collagen birefringence after picrosirius red staining of normal or RDEB ECM. Example images are shown above graph. (**b**) Graph shows mean percent increase comparing day 0 with day 7 for ECM engineered from separate normal and RDEB fibroblast populations. (**c**) The left panel shows an example of mean relative pixel intensity (± standard deviation) for a single normal fibroblast population. The right panel shows the percent increase in collagen after the addition of 5 ng of TGF-β compared with vehicle control after 7 days for three separate experiments using two separate populations. (**d**) Inhibition of TSP1 by a peptide inhibitor reduces collagen density in RDEB ECM. The graph shows the change in relative green or red pixel intensity after TSP1 peptide inhibitor (TSP-i) treatment *P < 0.05. For full details of the samples, see the extended legend in the Supplementary Materials online. Scale bar = 100 μm. CP, control peptide; d, day; RDEB, recessive dystrophic epidermolysis bullosa; TGF, transforming growth factor.
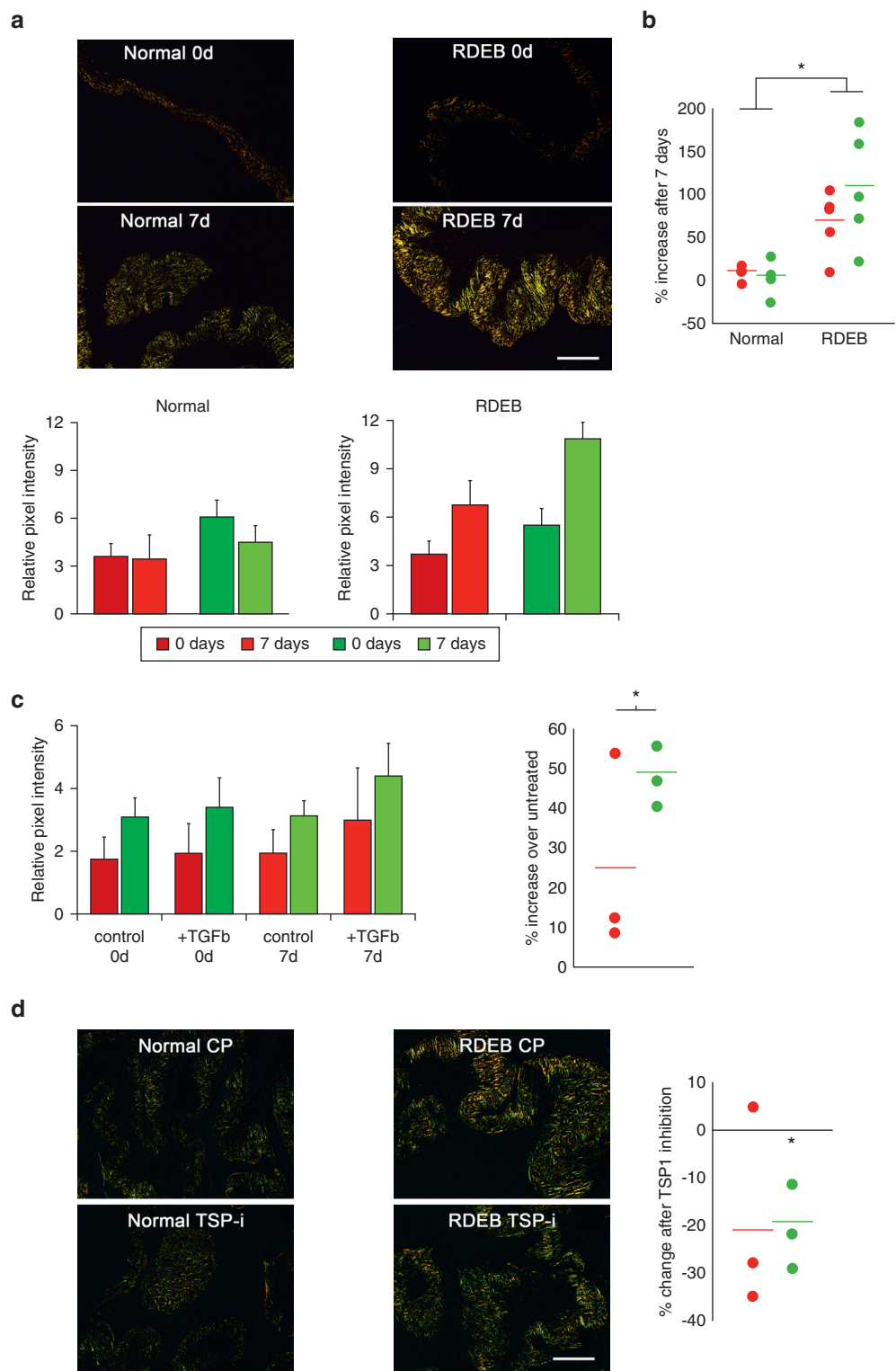
this protein will likely influence TSP1 activation of TGF-β. Further work will be required to clarify the relationship between these proteins in RDEB and to analyze other TGF-β–activating mechanisms. Furthermore, how the TGF-β ligand is bound and sequestered in RDEB ECM is unknown, and further work is necessary to fully understand the role of TGF-β in fibrosis of patient skin. We believe that altered protein secretion has a major impact on the ECM composition in RDEB, and we are actively pursuing this line of inquiry.

For a long time, C7 has been thought of as only a structural component, providing tensile strength to the epidermal-dermal junction (Burgeson, 1993), and certainly anti-C7 antibody binding in the skin is focused in this region (Leigh
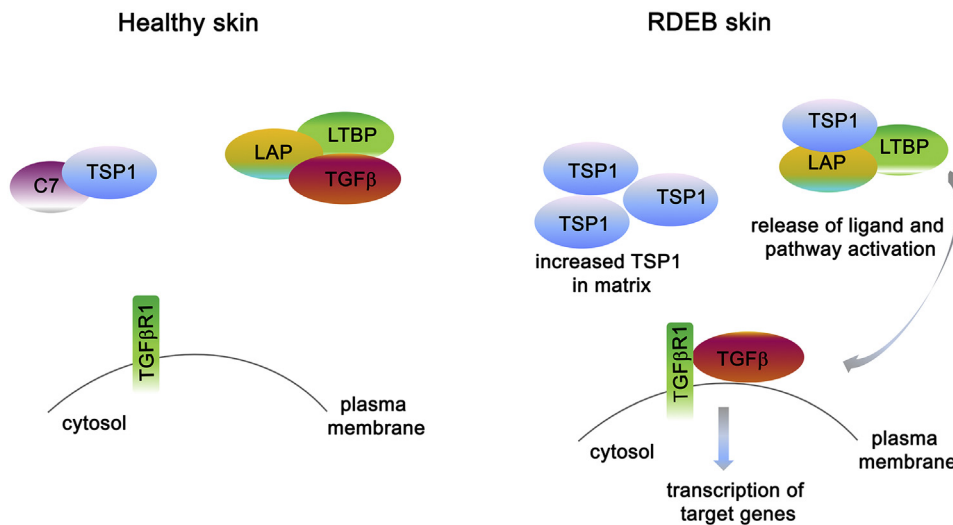
VS Atanasova et al.
C7, TSP1, and TGF-β Activation in RDEB

Figure 5. Proposed mechanism of TSP1-driven activation of TGF-β in RDEB skin. In healthy skin, TSP1 and C7 are bound, preventing TGF-β ligand release from the LAP/LTBP complex. In RDEB skin, C7 is missing, leading to increased TSP1 availability in the matrix, which triggers increased release of the TGF-β ligand from the latent complex followed by binding to cell surface TGF-β receptor type I and activation of downstream signaling.

et al., 1988). Emerging data, however, have begun to identify signaling roles for C7 in maintaining ECM homeostasis throughout the dermal layer, such as governing the levels of transglutaminase-2, an enzyme important for cross-linking ECM components (Kuttner et al., 2014). This study used proteomics to identify a number of C7 binding partners in dermal fibroblasts, including the enzyme lysyl hydroxylase-3, which is also involved in ECM cross-linking (Watt et al., 2015), but did not identify TSP1. The work described here clearly shows C7-TSP1 binding and highlights the possibility that further C7 binding partners may be uncovered in the future.

RDEB remains an intractable disorder with no cure. Multiple clinical trials have been reported that use various therapeutic approaches, including bone marrow transplantation (Wagner et al., 2010), cell-based therapy (Petrof et al., 2013), and grafting of gene-corrected keratinocytes (Siprashvili et al., 2016). Each of these approaches has focused on replacing C7, and yet progress here has been slow, although strategies to ameliorate symptoms in RDEB, such as wound healing, have emerged (Schwieger-Briel et al., 2017). Another such approach would be to inhibit TGF-β. However, global inhibition of this pathway has had limited success, likely because of its pleotropic and ubiquitous nature (Murphy-Ullrich and Suto, 2017). Nyström and colleagues (2015) recently showed preclinical efficacy of targeting the angiotensin II type I receptor in murine models of RDEB using the US Food and Drug Administration-approved drug losartan (Nyström et al., 2015). This approach indirectly targets TFG-β and has remarkable efficacy in reducing paw fibrosis in RDEB hypomorphic animals, suggesting that reducing TGF-β signaling in a targeted manner will also have clinical benefit. To this end, we identified TSP1 as a mediator of fibrosis in RDEB that can potentially be pharmacologically targeted to reduce TGF-β signaling in patients. In fact, a previous study in rat mesangial cells and rat cardiac fibroblasts showed that peptide inhibition of TSP1 blocked angiotensin II-induced TGF- β activation, suggesting a direct relationship with angiotensin II and placing TSP1 downstream in an angiotensin II—TSP1—TGF- β cascade (Zhou et al., 2006).

Therefore, targeting TSP1 may be more specific in the context of RDEB and would prevent global inhibition of TGF-β signaling, which has been shown to be associated with significant adverse effects (Connolly et al., 2011; Denton et al., 2007). Although this approach will not replace C7 in RDEB patients, it has the potential to ameliorate significant complications in this severe condition, and until we are able to find a curative therapy for this disease, we continue to explore evidence-based strategies to improve the quality of life for patients with RDEB.

MATERIALS AND METHODS

For full experimental details, see the Supplementary Materials online.

Cell culture

The cells used in this study were isolated from skin biopsy samples taken as routine surgical or diagnostic procedures. Informed written consent was obtained from each patient, and this study was performed in accordance with the Declaration of Helsinki and was approved by all participating institutional review boards. The cells were cultured at 37 °C with 5% CO_2, in DMEM (Corning Cellgro, Mediatech, Manassas, VA), which was supplemented with 10% fetal bovine serum (catalog no. PS-FB1; Peak Serum, Wellington, CO). Normal and RDEB fibroblasts were used up to passage 7.

Binding assay

A biosensor (SensiQ Pioneer; SensiQ Technologies, Oklahoma City, OK) was used to analyze TSP1/C7, TSP1/collagen IV, and TSP1/MMP9 binding interactions at 37 °C. For the C7/TSP1 binding assays, C7 was first bound to the chip surface (COOH1 SPR chip, SensiQ Technologies); carboxylate groups present on the surface were activated by injection of a 1:1 mixture of 0.1 mol/L N-hydroxysuccinimide and 0.4 mol/L N-Ethyl-3-(3-dimethylaminopropyl) carbodiimide (Thermo Fisher Scientific, Waltham, MA). Subsequently, 70 μg/ml of C7 in 10 mmol/L acetate buffer at pH 4.5 was allowed to bind to the activated surface until a response plateau was reached. The residual active groups were blocked by an injection of 100 μl of 1 mol/L Tris-HCl (pH 8.5). Subsequently, the chip was equilibrated with 4-(2-hydroxyethyl)-1-piperazineethanesulfonic acid (i.e., HEPES)-buffered saline

ARTICLE IN PRESS

VS Atanasova et al.
C7, TSP1, and TGF-β Activation in RDEB

containing 0.005% Tween 20 (HBS-TE). Excess non-bound material was removed by washing the chip with HBS-TE, followed by three consecutive washes with 10 mmol/L HCl.

For the TSP1/collagen IV and TSP1/MMP9 binding assays, TSP1 was first biotinylated with EZ-Link Sulfo-NHS-Biotin compound, according to the manufacturer's protocol (Thermo Fisher Scientific). Successful biotinylation was confirmed by Western blot of electrophoresed TSP1 and detected with the use of horseradish peroxidase conjugated to avidin. After biotinylation, TSP1 was immobilized on the Neutravidin-coated BioCap biosensor (Pall ForteBio, Menlo Park, CA).

To analyze the kinetic binding, a sensor chip was primed with HBS-TE for 10 minutes. Subsequently, the association phase was initiated by injecting a free analyte at a rate of 10 µl/minute for 20 minutes. After that time, the dissociation phase was initiated by injecting the analyte-free buffer. After each assay, the surface of the sensor chip was regenerated by washing with 10 mmol/L HCl, followed by equilibration with HBS-TE. During regeneration cycles, attention was paid to ensure that surface-bound analyte was completely removed, and the washing continued until a response equal to a baseline value was reached.

The following concentrations of free interactants were used: (i) for the TSP1/C7 binding assays, free TSP1 was added at concentrations ranging from 262 pmol/L to 67 nmol/L; (ii) for the TSP1/collagen IV binding assays, free collagen IV was added at concentrations ranging from 1 nmol/L to 240 nmol/L; (iii) for the TSP1/MMP9 binding assays, free MMP9 was added at concentrations ranging from 0.5 nmol/L to 130 nmol/L.

For all binding assays, data from the biosensor were analyzed by the global fitting method described by Myszka and Morton (1998). For each assay, the association rate constants (k_{on}) and the dissociation rate constants (k_{off}) were obtained, and the equilibrium dissociation constants (K_d) values were calculated from a ratio of k_{off}/k_{on}. Subsequently, the equilibrium association constant (K_a) values (termed *affinity*) were derived as the inverse of K_d. In all binding assays, bovine serum albumin-coated channel served as the reference.

Preparation of fibroblast-derived ECM and picrosirius red staining

Six-well plates were seeded at 1×10^5 cells/well and left to reach confluency. The medium was changed every other day with fresh 10% fetal bovine serum in DMEM and supplemented with 150 µmol/L L-ascorbic acid phosphate (catalog no. 013-12061; Wako, Richmond, VA). Matrices were detached from the tissue culture plastic using a 1-ml pipette tip and either collected immediately or left in suspension culture for 7 days before being collected and then fixed in 4% paraformaldehyde solution. The fixed matrices were embedded in 1% agarose gel and then in paraffin. For picrosirius red staining, each matrix was cut into 4–6-µm thick sections. After staining, the sections were analyzed with a polarizing microscope at ×20 magnification and 800-ms exposure time (Eclipse LV100POL; Nikon, Tokyo, Japan). Images were captured using NIS-elements software (Nikon).

Collagen quantification and statistical methods

To quantify collagen density, collected polarizing light microscopic images were analyzed in Adobe Photoshop CS6 (Adobe, San Jose, CA). For each individual red-green-blue color image, we overlaid a coherent single square lattice to produce a total of 221 test points (at a distance of 144 pixels). For every test point that intersected

collagen birefringence on each image, pixel density was measured in an area of 64×64 pixels for each of the green and red channels separately. The average pixel density across 3–5 separate images for each individual sample was recorded. Comparisons between conditions (normal vs. RDEB, TGF-β vs. vehicle, TSP1 (TSP1-i) vs. control peptide (CP)) were made only between experiments performed, processed, and analyzed at the same time. Paired two-tailed t test and two-tailed Mann-Whitney test were used for statistical analysis with Prism 8 (GraphPad Software, San Diego, CA).

ORCID
Julio C. Salas-Alanis: http://orcid.org/0000-0002-7307-3898

REFERENCES

Agah A, Kyriakides TR, Lawler J, Bornstein P. The lack of thrombospondin-1 (TSP1) dictates the course of wound healing in double-TSP1/TSP2-null mice. Am J Pathol 2002;161:831–9.

Aho S, Uitto J. Two-hybrid analysis reveals multiple direct interactions for thrombospondin 1. Matrix Biol 1998;17:401–12.

Bein K, Simons M. Thrombospondin type 1 repeats interact with matrix metalloproteinase 2. Regulation of metalloproteinase activity. J Biol Chem 2000;275:32167–73.

Brittingham R, Uitto J, Fertala A. High-affinity binding of the NC1 domain of collagen VII to laminin 5 and collagen IV. Biochem Biophys Res Commun 2006;343:692–9.

Burgeson RE. Type VII collagen, anchoring fibrils, and epidermolysis bullosa. J Invest Dermatol 1993;101:252–5.

Castle V, Varani J, Fligiel S, Prochownik EV, Dixit V. Antisense-mediated reduction in thrombospondin reverses the malignant phenotype of a human squamous carcinoma. J Clin Invest 1991;87:1883–8.

Connolly EC, Saunier EF, Quigley D, Luu MT, De Sapio A, Hann B, et al. Outgrowth of drug-resistant carcinomas expressing markers of tumor aggression after long-term TβRI/II kinase inhibition with LY2109761. Cancer Res 2011;71:2339–49.

Crawford SE, Stellmach V, Murphy-Ullrich JE, Ribeiro SM, Lawler J, Hynes RO, et al. Thrombospondin-1 is a major activator of TGF-β1 in vivo. Cell 1998;93:1159–70.

Daniel C, Schaub K, Amann K, Lawler J, Hugo C. Thrombospondin-1 is an endogenous activator of TGF-beta in experimental diabetic nephropathy in vivo. Diabetes 2007;56:2982–9.

Denton CP, Merkel PA, Furst DE, Khanna D, Emery P, Hsu VM, et al. Recombinant human anti-transforming growth factor β1 antibody therapy in systemic sclerosis: a multicenter, randomized, placebo-controlled phase I/II trial of CAT-192. Arthritis Rheum 2007;56:323–33.

Diegelmann RF, Evans MC. Wound healing: an overview of acute, fibrotic and delayed healing. Front Biosci 2004;9:283–9.

DiPietro LA, Nissen NN, Gamelli RL, Koch AE, Pyle JM, Polverini PJ. Thrombospondin 1 synthesis and function in wound repair. Am J Pathol 1996;148:1851–60.

ARTICLE IN PRESS

VS Atanasova et al.
C7, TSP1, and TGF-β Activation in RDEB

Fine JD, Johnson LB, Weiner M, Li KP, Suchindran C. Epidermolysis bullosa and the risk of life-threatening cancers: the National EB Registry experience, 1986–2006. J Am Acad Dermatol 2009;60:203–11.

Fritsch A, Loeckermann S, Kern JS, Braun A, Bosl MR, Bley TA, et al. A hypomorphic mouse model of dystrophic epidermolysis bullosa reveals mechanisms of disease and response to fibroblast therapy. J Clin Invest 2008;118:1669–79.

Galvin NJ, Vance PM, Dixit VM, Fink B, Frazier WA. Interaction of human thrombospondin with types I–V collagen: direct binding and electron microscopy. J Cell Biol 1987;104:1413–22.

Halder SK, Beauchamp RD, Datta PK. A specific inhibitor of TGF-beta receptor kinase, SB-431542, as a potent antitumor agent for human cancers. Neoplasia 2005;7:509–21.

Hugo C. The thrombospondin 1-TGF-β axis in fibrotic renal disease. Nephrol Dial Transplant 2003;18:1241–5.

Kuroki H, Hayashi H, Nakagawa S, Sakamoto K, Higashi T, Nitta H, et al. Effect of LSKL peptide on thrombospondin 1-mediated transforming growth factor β signal activation and liver regeneration after hepatectomy in an experimental model. Br J Surg 2015;102:813–25.

Kuttner V, Mack C, Gretzmeier C, Bruckner-Tuderman L, Dengjel J. Loss of collagen VII is associated with reduced transglutaminase 2 abundance and activity. J Invest Dermatol 2014;134:2381–9.

Kuttner V, Mack C, Rigbolt KT, Kern JS, Schilling O, Busch H, et al. Global remodelling of cellular microenvironment due to loss of collagen VII. Mol Syst Biol 2013;9:657.

Leigh IM, Eady RA, Heagerty AH, Purkis PE, Whitehead PA, Burgeson RE. Type VII collagen is a normal component of epidermal basement membrane, which shows altered expression in recessive dystrophic epidermolysis bullosa. J Invest Dermatol 1988;90:639–42.

Martins VL, Caley MP, Moore K, Szentpetery Z, Marsh ST, Murrell DF, et al. Suppression of TGFβ and angiogenesis by type VII collagen in cutaneous SCC. J Natl Cancer Inst 2016;108(1):djv293.

Merle B, Malaval L, Lawler J, Delmas P, Clezardin P. Decorin inhibits cell attachment to thrombospondin-1 by binding to a KKTR-dependent cell adhesive site present within the N-terminal domain of thrombospondin-1. J Cell Biochem 1997;67:75–83.

Mittapalli VR, Madl J, Loffek S, Kiritsi D, Kern JS, Romer W, et al. Injury-driven stiffening of the dermis expedites skin carcinoma progression. Cancer Res 2016;76:940–51.

Murphy-Ullrich JE, Mosher DF. Localization of thrombospondin in clots formed in situ. Blood 1985;66:1098–104.

Murphy-Ullrich JE, Suto MJ. Thrombospondin-1 regulation of latent TGF-β activation: a therapeutic target for fibrotic disease. Matrix Biol 2017;68–69:28–43.

Myszka DG, Morton TA. CLAMP: a biosensor kinetic data analysis program. Trends Biochem Sci 1998;23:149–50.

Ng YZ, Pourreyron C, Salas-Alanis JC, Dayal JH, Cepeda-Valdes R, Yan W, et al. Fibroblast-derived dermal matrix drives development of aggressive cutaneous squamous cell carcinoma in patients with recessive dystrophic epidermolysis bullosa. Cancer Res 2012;72:3522–34.

Ng YZ, South AP. Tissue engineering of tumor stromal microenvironment with application to cancer cell invasion. J Vis Exp 2014;85:51321.

Nyström A, Bruckner-Tuderman L. Injury- and inflammation-driven skin fibrosis: the paradigm of epidermolysis bullosa. Matrix Biol 2018;68–69:547–60.

Nyström A, Thriene K, Mittapalli V, Kern JS, Kiritsi D, Dengjel J, et al. Losartan ameliorates dystrophic epidermolysis bullosa and uncovers new disease mechanisms. EMBO Mol Med 2015;7:1211–28.

Nyström A, Velati D, Mittapalli VR, Fritsch A, Kern JS, Bruckner-Tuderman L. Collagen VII plays a dual role in wound healing. J Clin Invest 2013;123:3498–509.

Odorisio T, Di Salvio M, Orecchia A, Di Zenzo G, Piccinni E, Cianfarani F, et al. Monozygotic twins discordant for recessive dystrophic epidermolysis bullosa phenotype highlight the role of TGF-β signalling in modifying disease severity. Hum Mol Genet 2014;23:3907–22.

Petrof G, Martinez-Queipo M, Mellerio JE, Kemp P, McGrath JA. Fibroblast cell therapy enhances initial healing in recessive dystrophic epidermolysis bullosa wounds: results of a randomized, vehicle-controlled trial. Br J Dermatol 2013;169:1025–33.

Raugi GJ, Olerud JE, Gown AM. Thrombospondin in early human wound tissue. J Invest Dermatol 1987;89:551–4.

Resovi A, Pinessi D, Chiorino G, Taraboletti G. Current understanding of the thrombospondin-1 interactome. Matrix Biol 2014;37:83–91.

Ribeiro SM, Poczatek M, Schultz-Cherry S, Villain M, Murphy-Ullrich JE. The activation sequence of thrombospondin-1 interacts with the latency-associated peptide to regulate activation of latent transforming growth factor-β. J Biol Chem 1999;274:13586–93.

Rodriguez-Manzaneque JC, Lane TF, Ortega MA, Hynes RO, Lawler J, Iruela-Arispe ML. Thrombospondin-1 suppresses spontaneous tumor growth and inhibits activation of matrix metalloproteinase-9 and mobilization of vascular endothelial growth factor. Proc Natl Acad Sci USA 2001;98:12485–90.

Sato Y, Rifkin DB. Inhibition of endothelial cell movement by pericytes and smooth muscle cells: activation of a latent transforming growth factor-beta 1-like molecule by plasmin during co-culture. J Cell Biol 1989;109:309–15.

Schultz-Cherry S, Chen H, Mosher DF, Misenheimer TM, Krutzsch HC, Roberts DD, et al. Regulation of transforming growth factor-β activation by discrete sequences of thrombospondin 1. J Biol Chem 1995;270:7304–10.

Schultz-Cherry S, Lawler J, Murphy-Ullrich JE. The type 1 repeats of thrombospondin 1 activate latent transforming growth factor-beta. J Biol Chem 1994a;269:26783–8.

Schultz-Cherry S, Ribeiro S, Gentry L, Murphy-Ullrich JE. Thrombospondin binds and activates the small and large forms of latent transforming growth factor-beta in a chemically defined system. J Biol Chem 1994b;269:26775–82.

Schwieger-Briel A, Kiritsi D, Schempp C, Has C, Schumann H. Betulin-based oleogel to improve wound healing in dystrophic epidermolysis bullosa: a prospective controlled proof-of-concept study. Dermatol Res Pract 2017;2017:5068969.

Siprashvili Z, Nguyen NT, Gorell ES, Loutit K, Khuu P, Furukawa LK, et al. Safety and wound outcomes following genetically corrected autologous epidermal grafts in patients with recessive dystrophic epidermolysis bullosa. JAMA 2016;316:1808–17.

Streit M, Velasco P, Riccardi L, Spencer L, Brown LF, Janes L, et al. Thrombospondin-1 suppresses wound healing and granulation tissue formation in the skin of transgenic mice. EMBO J 2000;19:3272–82.

Wagner JE, Ishida-Yamamoto A, McGrath JA, Hordinsky M, Keene DR, Woodley DT, et al. Bone marrow transplantation for recessive dystrophic epidermolysis bullosa. N Engl J Med 2010;363:629–39.

Wang TN, Qian XH, Granick MS, Solomon MP, Rothman VL, Tuszynski GP. The effect of thrombospondin on oral squamous carcinoma cell invasion of collagen. Am J Surg 1995;170:502–5.

Watt SA, Dayal JH, Wright S, Riddle M, Pourreyron C, McMillan JR, et al. Lysyl hydroxylase 3 localizes to epidermal basement membrane and is reduced in patients with recessive dystrophic epidermolysis bullosa. PLoS One 2015;10(9):e0137639.

Yamaguchi Y, Mann DM, Ruoslahti E. Negative regulation of transforming growth factor-beta by the proteoglycan decorin. Nature 1990;346(6281):281–4.

Yu Q, Stamenkovic I. Cell surface-localized matrix metalloproteinase-9 proteolytically activates TGF-β and promotes tumor invasion and angiogenesis. Genes Dev 2000;14:163–76.

Zhao C, Isenberg JS, Popel AS. Human expression patterns: qualitative and quantitative analysis of thrombospondin-1 under physiological and pathological conditions. J Cell Mol Med 2018;22:2086–97.

Zhou Y, Poczatek MH, Berecek KH, Murphy-Ullrich JE. Thrombospondin 1 mediates angiotensin II induction of TGF-β activation by cardiac and renal cells under both high and low glucose conditions. Biochem Biophys Res Comms 2006;339:633–41.

ARTICLE IN PRESS

VS Atanasova et al.
C7, TSP1, and TGF-β Activation in RDEB

SUPPLEMENTARY MATERIALS AND METHODS

Protein quantification

Protein concentration in cell lysates was assayed with Pierce bicinchoninic assay Protein Assay kit (Thermo Fisher Scientific). Samples containing 35 µg of protein were loaded onto SDS-PAGE gel for detection of thrombospondin 1, C7, phosphorylated smad3, and smad2/3. For detection of GAPDH, samples containing 4 µg protein were loaded onto gels.

Recombinant C7 herpes simplex virus 1 delivery

RDEB or normal breast dermal fibroblasts were seeded onto a six-well plate 1 day before infection. On the day of infection, the cells were trypsinized and counted, and a multiplicity of infection of 0.1 was used. The virus was kept for a total of 2 hours, after which the cells were recovered with 10% fetal bovine serum DMEM medium supplemented with 150 µmol/L L-ascorbic acid phosphate (catalog no. 013-12061, Wako). The lysate of the cells was collected 48 hours after infection followed by Western blot analysis.

Quantitative reverse transcriptase–PCR

RNA was extracted from patient cells using the RNeasy Mini Kit (Qiagen, Hilden, Germany) according to the manufacturer's instructions. RNA samples were quantified with a NanoDrop Spectrophotometer (Thermo Fisher Scientific) and 1.5 µg RNA was used for preparation of cDNA using SuperScript III First-Strand Synthesis System (Invitrogen, Carlsbad, CA). For detection of *TSP1* expression, we used the following primers: forward primer, TTGTCTTTGG AACCACACCA, and reverse CTGGACAGCTCATCACAGGA. For *GAPDH* amplification, the following primers were used: forward, CTGGGCTACACTGAGCACC, and reverse AAGTGG TCGTTGAGGGCAATG. For the quantitative PCR reaction, SYBR Select Master mix (Life Technologies, Carlsbad, CA) was used, and the template cDNA samples were diluted 1:25. Experiments were performed in triplicate.

Small interfering RNA knockdown of TSP1 and Western blot analysis

For small interfering RNA knockdown of TSP1, 1.3×10^5 fibroblasts were plated in six-well plates. The next day, the cells were transfected with SMARTpool:ON-TARGETplus THBS1 (catalog no. L-019743-00-0005, 5 nmol) or ON-TARGETplus nontargeting control (catalog no. L-001810-10-05, Dharmacon, Lafayette, CO), using siLentFect Lipid (catalog no. 170-3361, BioRad, Hercules). After 6 hours of transfection, the cells were recovered with DMEM (Corning Cellgro) supplemented with 10% fetal bovine serum (catalog no. PS-FB1, Peak Serum). After 48 hours, cells were lysed with radio-immunoprecipitation assay buffer (i.e., RIPA) and scraped from the plates, followed by 5 minutes of centrifugation at 4 °C. For detection of TSP1, 35-µg protein samples were loaded on a 8% acrylamide gel. Primary antibodies used were monoclonal mouse antibody raised against TSP1 (sc-59887; Santa Cruz Biotechnology, Dallas, TX) (dilution 1:1,000), rabbit monoclonal anti phospho-smad3 (ab52903; Abcam, Cambridge, UK) (dilution 1:1,000), rabbit polyclonal anti smad2/3 antibody (catalog no. 3102; Cell Signaling Technology, Danvers, MA), and monoclonal mouse anti-GAPDH antibody (sc-365062,

Santa Cruz Biotechnology) (dilution 1:5,000). Resolved proteins were transferred onto nitrocellulose membrane with a BioRad Trans-Blot-Turbo, blocked in phosphate buffered saline with Tween 20 (0.1% Tween), 5% milk, or 5% bovine serum albumin, according to requirements of the primary antibody, and incubated overnight with the primary antibody. After incubation with IgG-horseradish peroxidase–conjugated secondary antibody (Santa Cruz Biotechnology), membrane was incubated with ECL Western blotting substrate (Thermo Fisher Scientific) and exposed to CL-X Posure X-ray film (Thermo Fisher Scientific).

Co-immunoprecipitation

Co-immunoprecipitation was performed with 4C5, anti-DDK Agarose Immunoprecipitation Kit AR100023 from OriGene Technologies (Rockville, MD) following the manufacturer's instructions. Briefly, RDEB fibroblasts not expressing C7 were transduced with HSV1 viral backbone–C7-DDK–tagged virus at multiplicity of infection 0.1. After recovery, the cells were grown for 48 hours in the presence of L-ascorbic acid 150 µmol/L. For immunoprecipitation of C7, the lysates were incubated with anti-DDK beads overnight on a rotor, washed three times with $1\times$ washing buffer, mixed with $2\times$ loading buffer and prepared for SDS-PAGE gel analysis.

Proximity ligation assay

Proximity ligation assay was performed using Duolink In Situ Red Starter Kit Mouse/Rabbit Non-Haz (Duo92101; Sigma-Aldrich, St. Louis, MO) according to the manufacturer's protocol. In brief, normal human fibroblasts were plated onto coverslips in 24-well plates at 0.5×10^5 cells/well. The cells were fixed with 4% paraformaldehyde and blocked for 1 hour at 37 °C and then with the respective antibodies for 1 hour. After amplification of the signal, the slides were mounted and analyzed with a fluorescence microscope (EVOS FL Auto Imaging system, Thermo Fisher Scientific).

Immunohistochemistry

Six-micron sections were cut from samples frozen in optimal cutting temperature compound (OCT; Sakura Finetek, Torrance, CA) with a cryostat and fixed with 50:50 methanol:acetone mixture for 20 minutes. Slides were rehydrated with $1\times$ phosphate buffered saline for 5 minutes, followed by blocking for 20 minutes with phosphate buffered saline/0.1% Tween 20/3% bovine serum albumin (Sigma-Aldrich). Primary antibodies (ab85762, Abcam; 1:100 dilution and MAB3412; Millipore, Billerica, MA; 1:100 dilution) were incubated for 1.5 hours at room temperature. Secondary antibodies Alexa Fluor 594 goat anti-rabbit (1:800) (Invitrogen, Eugene, OR) and Alexa Fluor 488 goat anti-mouse (1:250, Invitrogen) were applied for 1 hour at room temperature. Slides were coverslipped with hard-set DAP I(Vector Labs, Burlingame, CA) and examined by fluorescence microscopy (EVOS FL Cell Imaging System, Thermo Fisher Scientific).

### TGF-β and peptide treatment of fibroblast-derived ECM

Matrices had the following treatments: control peptide SLLK, (AS-60875; AnaSpec, Fremont, CA) or LSKL thrombospondin 1 inhibitor (AS-60877, Anaspec) at 20 µmol/L; SB431542 TGF-beta inhibitor 1 µmol/L (S-1067; Selleckchem, Houston,

ARTICLE IN PRESS

VS Atanasova et al.
C7, TSP1, and TGF-β Activation in RDEB

TX); TGF-β ligand (240-B-002; R&D Systems, Minneapolis, MN) at 2 ng/ml.

Figure 1 (extended legend). TGF-β signaling and TSP1 are up-regulated in RDEB. (**a**) Phosphorylated smad3 (PO$_4$-SMAD3) is increased in RDEB (left, RDEB84 and right, RDEB86) and RDEB SCC fibroblasts (left to right: RDEB71, RDEB70, and RDEB55) compared with normal human fibroblasts (left to right: Br11, Br10, and Br9). The graph shows densitometry quantification of phosphorylated SMAD3 (PO$_4$-SMAD3) for each given population. (**b**) Expression of TSP1 is increased in RDEB versus normal controls at transcript (graph, top left) and protein (Western blot panel, bottom right and immunohistochemistry panels, right) levels. Graph (left) shows quantitative PCR levels of TSP1 relative to GAPDH in three separate normal fibroblast populations (FS1, FS2, FS3) compared with four different RDEB populations (RDEB75, RDEB79, RDEB80, and RDEB73). Western blot data (bottom left) compares two normal cell populations (Br43 and Br48) with one RDEB and one RDEB SCC cell population (RDEB75 and RDEB106). Six-micrometer frozen sections were processed and incubated with an antibody raised against TSP1 (ab85762, Abcam) (red, left) and the nuclear stain DAPI (blue, right) using normal breast tissue (Br53), RDEB SCC tissue (RDEB119), and corresponding perilesional tissue (RDEB). Images show a 400 × 400-μm region of either the dermis or SCC stroma. The signal in regions of the image for RDEB SCC that was positive for keratin has been removed to show TSP1 in the stroma only; original images and corresponding regions are presented in Supplementary Figure S2. (**c**) Levels of phosphorylated SMAD3 relative to GAPDH correlate with TSP1. Western blot data compares one normal cell population (Br61) with five RDEB normal cell populations (from four patients; left to right: RDEB85, RDEB86, RDEB119-8, RDEB119-11, and RDEB118). The graph shows quantification of Western blotting relative to GAPDH plotting TSP1 (*x*-axis) against phosphorylated SMAD3 (*y*-axis). (**d**) Re-expression of C7 in RDEB fibroblasts from four different patients (left to right: RDEB70, RDEB71, RDEB81, and RDEB84) results in decreased intracellular and increased extracellular TSP1 compared with control. (**e**) TSP1 mRNA levels do not change 48 hours after expression of recombinant C7. The graphs shows quantitative PCR levels of (left) TSP1 or (right) COL7A1 48 hours after delivery of recombinant C7 (C7) or control vector (Control) for two populations of normal human fibroblasts (Br23 and Br43), RDEB SCC fibroblasts (RDEB70 and RDEB71), and RDEB fibroblasts (RDEB82 and RDEB84). *$P < 0.05$. NHF, normal human fibroblast; RDEB, recessive dystrophic epidermolysis bullosa; SCC, squamous cell carcinoma; TGF, transforming growth factor.

Figure 4 (extended legend). RDEB engineered ECM exhibits increased collagen content compared with normal ECM and can be reduced with a peptide inhibitor of TSP1-LAP binding. (**a**) RDEB SCC (RDEB71F) ECM exhibits smad3 increased collagen synthesis after 7 days of remodeling in suspension culture compared with normal fibroblast (Br10 and Br11) ECM. Scale bar graph shows mean relative pixel intensity (± standard deviation) for either the green or red channel from areas of images positive for collagen birefringence after picrosirius red staining. Data show an increase of collagen fiber density in RDEB matrices after 7 days. (**b**) The graph shows mean percent increase comparing day 0 with day 7 for four separate normal fibroblast populations (circles; Br10, Br31, Br37, and Br27) and five separate RDEB fibroblast populations (circles; RDEB71 [SCC], RDEB74, RDEB75, RDEB77, and RDEB81). RDEB fibroblasts show significantly greater percent increase in collagen density after 7 days when compared with normal fibroblasts. (**c**) TGF-β stimulation of normal cell matrices increases collagen density after 7 days. The graph on the left shows an example of mean relative pixel intensity (± standard deviation) for a single population (Br31), and the graph on the right shows the percent increase in collagen after addition of 5 ng of TGF-β compared with vehicle control after 7 days for three separate experiments using two separate donor populations (Br31 and Br32). (**d**) Inhibition of TSP1 by a peptide inhibitor reduces collagen density in RDEB ECM. Circles show change in relative pixel intensity for individual samples, and bar shows mean. *$P < 0.05$. d, day; RDEB, recessive dystrophic epidermolysis bullosa; TGF, transforming growth factor.

ARTICLE IN PRESS

VS Atanasova et al.
C7, TSP1, and TGF-β Activation in RDEB
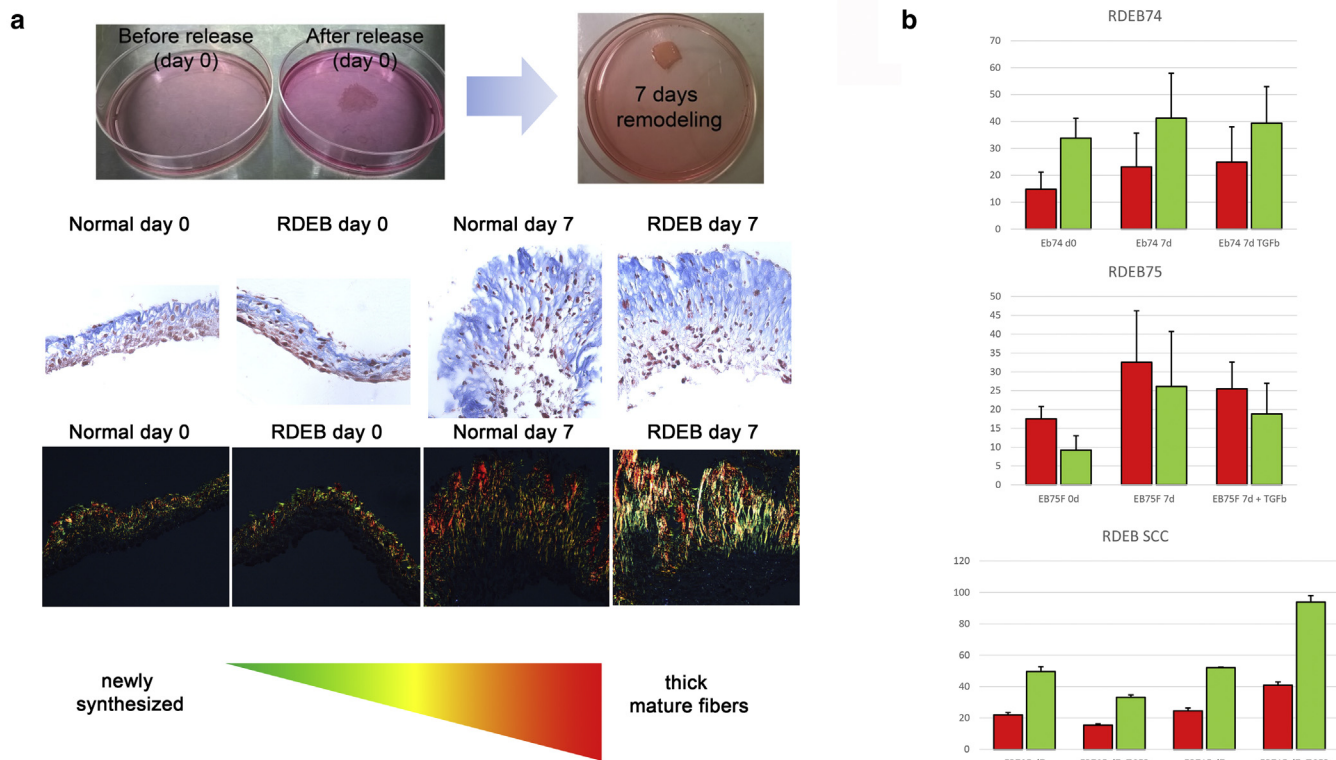
Supplementary Figure S1. Engineered extracellular matrix identifies pathological changes in RDEB fibroblasts. (a) Primary fibroblasts isolated from controls (Normal, Br10/11F) or RDEB patients (RDEB, RDEB71) were allowed to grow for a period of time (1–3 weeks) until the ECM containing fibroblasts could be detached from tissue culture plastic (day 0) and allowed to remodel in suspension for a period of 7 days (day 7) (top row). Engineered ECM was then formalin fixed and paraffin embedded before histological analysis. Trichrome blue staining identified the collagen content of engineered ECM (second row), and picrosirius red staining and subsequent imaging under polarized light captured collagen birefringence (third row), which is indicative of collagen fibril thickness. The illustration at the bottom shows green, which represents newly synthesized thin fibrils, progressing to red, which represents mature, thicker fibrils. (**b**) Quantification of relative pixel density measuring green and red pixels in a given image identified little change in collagen content after TGF-β stimulation (2 ng/ml) in three out of four RDEB primary fibroblasts. Graphs show mean pixel intensity, and error bars represent mean ± standard deviation. d, day; ECM, extracellular matrix; RDEB, recessive dystrophic epidermolysis bullosa; SCC, squamous cell carcinoma; TGF, transforming growth factor.

ARTICLE IN PRESS

VS Atanasova et al.
C7, TSP1, and TGF-β Activation in RDEB
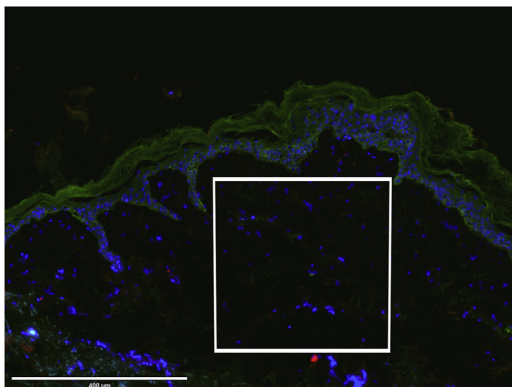
a Normal Breast

b RDEB peri-lesional skin
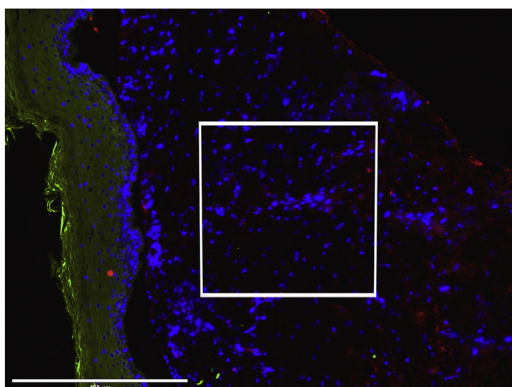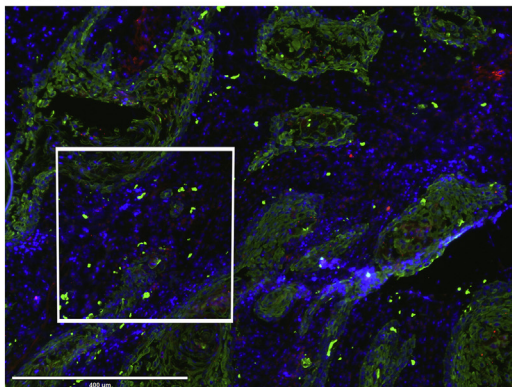
c RDEB SCC

Supplementary Figure S2. TSP1 protein is increased in the dermis of RDEB skin and the stroma of RDEB SCC compared with normal breast skin. (**a**) Normal breast skin. (**b**) RDEB perilesional skin. (**c**) RDEB SCC. Six-micrometer frozen sections were processed and incubated with antibodies raised against TSP1 (no. ab85762, Abcam) (1:100 dilution) (red) and Cytokeratin (no. MAB3412, Millipore) (1:100 dilution) (green) and mounted in media containing the nuclear stain DAPI (blue). White boxes depict regions selected for presentation in Figure 1b. Scale bars = 400 μm. RDEB, recessive dystrophic epidermolysis bullosa; SCC, squamous cell carcinoma.

ARTICLE IN PRESS

VS Atanasova et al.
C7, TSP1, and TGF-β Activation in RDEB

Supplementary Table S1. Patient cells used in this study

Diagnosis	Cell Name	Mutation	Patient Age in Years	Sex	Body Site
Healthy	Br3	N/A	80	Female	Breast
Healthy	Br5	N/A	54	Female	Breast
Healthy	Br10	N/A	54	Female	Breast
Healthy	Br11	N/A	48	Female	Breast
Healthy	Br27	N/A	24	Female	Breast
Healthy	Br31	N/A	28	Female	Breast
Healthy	Br37	N/A	23	Female	Breast
Healthy	Br43	N/A	33	Female	Breast
Healthy	Br46	N/A	23	Female	Breast
Healthy	Br48	N/A	22	Female	Breast
Healthy	Br53	N/A	22	Female	Breast
Healthy	Br61	N/A	20	Female	Breast
Healthy	FS1-3	N/A	<1	Male	Foreskin
RDEB-SG	RDEB55	c.8440C>T (p.R2814X)/c.8440C>T (p.R2814X)	28	Male	SCC, left outer ankle
RDEB-SG	RDEB70	c.425A>G (p.K142R)/c.425A>G (p.K142R)	27	Male	SCC metastasis, left elbow
RDEB-SG	RDEB71	c.IVS34-1G>A/c.3840delC (p.G1281VfsX44)	35	Female	SCC, left hand
RDEB-SG	RDEB99	c.6527dupC (p.G2177WfsX113)/c.5532+1G>T	24	Male	SCC, back
RDEB-OG	RDEB73	c.2471dupG (p.G824fs)/c.2471dupG (p.G824fs)	46	Female	Armpit
RDEB-OG	RDEB74	c.2471dupG (p.G824fs)/c.2471dupG/p.G824fs	47	Female	Armpit
RDEB-SG	RDEB75	Not found	6	Female	Arm
RDEB-SG	RDEB77	c.2782insGACAC (p.Thr928Argfs*7)/c.2782insGACAC (p.Thr928Argfs*7)	13	Female	Arm
RDEB-SG	RDEB79	c.2471dupG (p.G824fs)/c.2471dupG (p.G824fs)	39	Female	Arm
RDEB-SG	RDEB80	c.2471dupG (p.G824fs)/c.2471dupG (p.G824fs)	41	Male	Arm
RDEB-SG	RDEB81	c.2923_2924insA (p.A975fs)/not found	29	Female	Arm
RDEB-SG	RDEB84	c.8697del11 (p.S2900Lfs*20)/c.8697del11 (p.S2900Lfs*20)	2	Male	Arm
RDEB-OG	RDEB86	Not found	3	Female	arm
RDEB-SG	RDEB118	c.1732C>T (p.Arg578*)/c.7474C>T (p.Arg2492*)	37	Female	SCC, leg
RDEB-SG	RDEB119	c.5565_5568+8delinsA/c.6527insC (p.G2177WfsX113)	39	Female	SCC, leg
RDEB-SG	RDEB106F	c.5532+1G>T/c.3264_5293del (p.Q1089_G1764fsX7)	50	Male	SCC, back

Abbreviations: N/A, not applicable; OG, other generalized; RDEB, recessive dystrophic epidermolysis bullosa; SCC, squamous cell carcinoma; SG, severe generalized.